



ARTICLE

Population pharmacokinetic and exposure–response analyses of intravenous and subcutaneous rituximab in patients with chronic lymphocytic leukemia

Ekaterina Gibiansky¹ | Leonid Gibiansky¹ | Clarisse Chavanne² | Nicolas Frey² | Candice Jamois²

¹QuantPharm LLC, North Potomac, Maryland, USA

²Roche Innovation Center Basel, Basel, Switzerland

Correspondence

Candice Jamois, Roche Innovation Center Basel, Postfach, CH-4070, Basel, Switzerland.

Email: candice.jamois@roche.com

Funding information

The SAWYER and REACH studies, and the present pharmacokinetic analysis, were funded by F. Hoffmann-La Roche Ltd.

Abstract

A subcutaneous formulation of the anti-CD20 antibody rituximab has been developed. Fixed-dose subcutaneous rituximab delivers noninferior serum trough concentrations (C_{trough}), ensuring similar target saturation and comparable efficacy/safety, to intravenous rituximab, but with simplified and shortened preparation and administration. We aimed to characterize the pharmacokinetic (PK) and exposure–response properties of subcutaneous rituximab. Data from two clinical trials were analyzed to describe PKs and pharmacodynamics in patients with chronic lymphocytic leukemia following intravenous and subcutaneous rituximab administration. Intravenous and subcutaneous rituximab were described by a linear two-compartment population PK model with time-dependent and time-independent clearances, and first-order subcutaneous absorption. Main covariates influencing exposure were body size and baseline white blood cell count. Occurrence of adverse events was not correlated with rituximab exposure. Although greater and more sustainable B-cell depletion was observed with higher exposure, inherent limitations to the data (use of one dose level, and time-dependent and target-impacted PKs) prevented reliable assessment of exposure–response relationships.

Study Highlights

WHAT IS THE CURRENT KNOWLEDGE ON THE TOPIC?

Subcutaneous rituximab delivers noninferior serum trough concentrations (C_{trough}), ensuring similar target saturation and comparable efficacy and safety, to the intravenous formulation, but with simplified, shortened drug preparation and administration.

WHAT QUESTION DID THIS STUDY ADDRESS?

Although population pharmacokinetic (PK) models for rituximab have been described, the PK properties of the subcutaneous formulation versus intravenous rituximab remained to be fully described.

This is an open access article under the terms of the Creative Commons Attribution-NonCommercial-NoDerivs License, which permits use and distribution in any medium, provided the original work is properly cited, the use is non-commercial and no modifications or adaptations are made.

© 2021 Roche Diagnostics Corp. *CPT: Pharmacometrics & Systems Pharmacology* published by Wiley Periodicals, Inc. on behalf of the American Society for Clinical Pharmacology and Therapeutics

WHAT DOES THIS STUDY ADD TO OUR KNOWLEDGE?

Both rituximab formulations are described by a linear two-compartment population PK model with time-dependent and time-independent clearances, and first-order subcutaneous absorption, in patients with chronic lymphocytic leukemia (CLL). Rituximab exposure was not associated with safety, and variability in exposure was not associated with clinical response in the majority of patients.

HOW MIGHT THIS CHANGE DRUG DISCOVERY, DEVELOPMENT, AND/OR THERAPEUTICS?

Our analyses establish the population PK characteristics of rituximab following subcutaneous administration. There are no concerns relating to safety, clinical response, or anti-CD20 activity associated with switching to the subcutaneous route in patients with CLL.

INTRODUCTION

The type I anti-CD20 monoclonal antibody (mAb), rituximab, revolutionized the treatment of B-cell malignancies, including chronic lymphocytic leukemia (CLL)¹; addition of rituximab to chemotherapy significantly increased time to disease progression and overall survival in previously untreated (1L) and relapsed/refractory patients.^{2–4} First infusions of the original intravenous rituximab formulation (R-i.v.) are administered slowly over 3.5–4 h to minimize risk of potentially severe infusion reactions. A subcutaneous formulation of rituximab and recombinant human hyaluronidase (R-s.c.)⁵ has exhibited similar efficacy and safety, with noninferior pharmacokinetics (PKs), to R-i.v. in non-Hodgkin lymphoma and CLL.^{5–9} R-s.c. can be administered over 5–7 min, with 15 min of monitoring.¹⁰ Studies demonstrate patient satisfaction and healthcare practice efficiency advantages for R-s.c. versus R-i.v.^{11,12}

R-s.c. is approved in the United States and Europe with chemotherapy for patients with 1L or treated CLL, diffuse large B-cell lymphoma (DLBCL), and 1L follicular lymphoma (FL), and as monotherapy for relapsed/refractory FL and for maintenance in patients with FL responding to initial chemoimmunotherapy.^{10,13} United States approval in 2017 followed an Oncology Advisory Drug Committee review of the clinical development program, which assumed that attaining at least equivalent minimum steady-state serum rituximab exposure (trough plasma concentration [C_{trough}]) following R-s.c. and R-i.v. administration would result in the same degree of target saturation, and therefore comparable efficacy. The US Food and Drug Administration (FDA) approval in CLL was based upon the data reported herein.

The current analysis aimed to characterize further the PK properties of R-i.v. and R-s.c., identify covariate factors influencing rituximab's disposition, and explore exposure–response (ER) relationships in patients with CLL, utilizing data from the pivotal registrational trials for R-s.c.

METHODS

Population PK analysis

Prior development of population PK model

The population PK (PopPK) model utilized in the current analysis was developed previously using clinical data from two international, open-label, randomized controlled studies (Table 1): the two-part, phase Ib SAWYER study (NCT01292603) of fludarabine and cyclophosphamide (FC) plus R-s.c. or R-i.v. in 1L CLL^{8,9}; and the phase III REACH study (NCT00090051) of FC alone versus FC plus R-i.v. in previously treated CLL.⁴

Rituximab was given for six 28-day cycles:

- Intravenous (REACH, SAWYER): cycle (C) 1 375 mg/m², C2–6 500 mg/m²;
- Subcutaneous-1 (SAWYER part 1): C1–5 i.v., C6 various s.c. doses up to 2200 mg;
- Subcutaneous-2 (SAWYER part 2): C1 375 mg/m² i.v., C2–6 1600 mg s.c.

PK serum sampling schedules for both studies are detailed in Table 1 and Figure S1. Serum rituximab concentrations were determined using a validated sandwich enzyme-linked immunosorbent assay; values below the lower limit of quantification (LLOQ; 0.5 µg/ml; $n = 348$, 7.3%) were excluded.

The previously published initial model, based upon PK data from REACH, described rituximab PKs¹⁴ by a linear two-compartment model with clearance composed of a non-specific time-independent (CL_{inf}) term, associated with catabolic antibody clearance, and a time-dependent (CL_T) term, associated with target-mediated drug elimination (TMDD), which decreases exponentially over time:

$$CL = CL_T \cdot \exp(-k_{\text{des}} \cdot t) + CL_{\text{inf}}$$

where k_{des} is the rate constant of decay of CL_T with time (t).

TABLE 1 Summary of the two rituximab studies included in the PK analysis

Study	R administration route/dosing regimens ^a	PK measurements
SAWYER (BO25341) Phase Ib, two-part (Assouline et al.) ^{8,9} PK analysis: 4158 samples (2381 i.v., 1777 s.c.) from 234 patients (previously untreated CLL)	Part 1 (dose finding) R 375 mg/m ² i.v. C1, 500 mg/m ² i.v. C2–5, then 1400, 1600, or 1870 mg ^b s.c. C6 Part 2 (randomized) R 375 mg/m ² i.v. C1, then 500 mg/m ² i.v. C2–6 or R 375 mg/m ² i.v. C1, then 1600 mg ^c s.c. C2–6	Part 1 C5: predose, EOI, 1, 4, 10, and 14 days postdose C6: predose, 1, 2, 4, 10, 14, 28, and 56 days postdose Part 2 (both i.v. and s.c. arms) C1: predose, EOI, 1, 2, 7, and 14 days postdose; C2: predose and 14 days postdose C3–5: predose C6: predose, 1, 2, 7, 14, 28, and 56 days postdose Part 2 (i.v. arm only) C4 and C6: Additional samples collected EOI Part 2 (s.c. arm only) C2: Additional samples collected 1, 2, and 7 days postdose
REACH (BO17072) Phase III (Robak et al.) ⁴ PK analysis: 581 samples from 21 patients (previously treated CLL)	R: 375 mg/m ² i.v. (C1), then 500 mg/m ² i.v. (C2–6)	C1, C3, and C6: predose, 8, 11, and 24 h postdose, 3, 5, 7, 14, 21, and 28 days postdose Months 7, 8, 9, and 12

C, cycle(s); CLL, chronic lymphocytic leukemia; EOI, end of infusion; FC, fludarabine and cyclophosphamide; PK, pharmacokinetic; R, rituximab.

^aAll R dosing regimens were based on 28-day cycles and included FC chemotherapy. Recommended FC doses were 25 mg/m² + 250 mg/m² i.v. for 3 days every 28 days in both SAWYER and REACH, although equivalent oral therapy was also permitted in accordance with local practice and guidelines in SAWYER.

^bInitial maximum s.c. dose; subsequently adjusted on the basis of intermediate analyses up to a maximum of 2200 mg.

^cDetermined from part 1 of the study.

Subsequently, this model was updated with data from SAWYER part 1 (dose escalation) to suggest a s.c. dose for SAWYER part 2 that would match or exceed the rituximab exposure (C_{trough} on C6) seen with the i.v. 500 mg/m² regimen.⁹

Base PopPK model development

In the current analysis, the previous model was developed further with SAWYER part 2 data to confirm if the proposed 1600 mg s.c. dose could provide C_{trough} during C2–6 at least equivalent to i.v. dosing. Structural model refinement (Table S1) was data-driven and based on goodness-of-fit diagnostic plots, precision and plausibility of parameter estimates, minimum objective function value, and number of estimated parameters. An exponential error model in log-transformed variables with a concentration-dependent variance was used, which allows the residual variability to be higher at low concentrations, and is more robust than a commonly used combined additive and proportional error model (Supplementary Information).

Covariate model development

Covariates' (body weight, body surface area [BSA], body mass index [BMI], sex, age, baseline white blood cell count [WBC], tumor size [BSIZ], serum albumin concentration [BALB], and

presence of anti-drug antibodies [ADAs]) interactions with PK parameters were identified by scientific interest, mechanistic plausibility, and exploratory graphics, and included in covariate model development (Table S2). Less physiologically relevant markers were explored graphically only.

Model interpretation and refinement were based on point estimates, confidence intervals (CIs), and diagnostic plots of the covariate effects. Precisely estimated but clinically insignificant effects and those not supported by data (e.g., effects close to null value, with high relative standard error [RSE] or CIs including the null value) were excluded.

Model evaluation

Base and final PK models were evaluated using goodness-of-fit plots, simulated prediction-corrected visual predictive checks (VPC),^{15–17} and the normalized prediction distribution errors (NPDEs) procedure.^{18,19} For estimates of precision, asymptotic RSEs, 95% CIs, and nonparametric bootstrap 95% CIs²⁰ were obtained for each model parameter. Details are provided in the Supplementary Information.

Model-based simulations

The final PopPK model was used to simulate expected R-i.v. and R-s.c. concentration–time courses for the

proposed CLL dosing regimen, using individual covariates and parameters from 140 patients from SAWYER part 2. The simulations were used to evaluate the effect of covariates, determine the spread of concentrations and approach to steady-state at the end of C6, and compute PK parameters at C6, including area under the concentration–time curve over one cycle (AUC_{τ}), peak concentration (C_{max}), and C_{trough} . Clinically relevant covariates' effects were illustrated by comparing median concentrations and 90% prediction intervals over time.

PopPK analysis software

PopPK analysis was conducted using nonlinear mixed-effects modeling with NONMEM version 7.3.0 (ICON Development Solutions, Ellicott City, MD, USA). First-order conditional estimation with the INTERACTION option was used.

Exposure–safety and exposure–response analyses

Patient data from SAWYER part 2 were used to analyze exposure–safety and ER relationships (R-i.v., $n = 87$; R-s.c., $n = 86$).

Exposure–safety

The relationship between observed rituximab concentrations and serious adverse events (SAEs) was analyzed for system organ classes showing 4 or more SAEs in the PK database. Blood and lymphatic system disorders were investigated using the relationship between rituximab exposure and National Cancer Institute Common Toxicity Criteria for Adverse Events (NCI-CTCAE) grade of neutropenia. Cumulative AUC up to occurrence of each SAE and mean rituximab concentration (C_{mean}) were plotted for both treatment arms. Exposure measures were computed using dosing history and individual PK parameters from the final PopPK model. C_{mean} was defined as cumulative AUC until time to the last dose +28 days (DUR_{trt}) divided by DUR_{trt} .

C_{mean} distributions for subjects with no grade 3 or higher adverse events (AEs), grade 3 AEs, and grade 4 AEs were compared separately for R-i.v. and R-s.c. Relationships between rituximab exposure and time course of neutrophil counts were assessed using predicted C_{mean} values (computed as for SAEs). Patients were assigned to high, medium, or low exposure categories (C_{mean} tertiles). C_{mean} distributions for maximum neutropenia grades in each treatment arm were also evaluated.

Exposure–response

Tumor response (best overall response [BOR]) and B-cell counts were related to rituximab exposure using C_{mean} and C_{trough} values (at DUR_{trt}). BOR was based on a data snapshot of May 7, 2014.

Relationships between exposure, administration route, patient characteristics, or disease-specific covariates and progression-free survival (PFS) were explored using Kaplan–Meier (KM) plots stratified by administration route and exposure groups (e.g., tertiles). To consider potential confounding factors and compare the relationship between rituximab exposure and PFS following i.v. and s.c. dosing, an ER analysis of PFS was performed in patients who received all six doses of rituximab in SAWYER part 2 using semiparametric Cox proportional hazards (CPH) modeling. Models with linear, logarithmic, E_{max} , and step-like functions of exposure were investigated. Univariate covariate screening was performed first to identify covariates for incorporation (Table S3). Forward addition followed by backward elimination procedures were used to find the best covariate model. The Bayesian Information Criterion (BIC) was used for model discrimination. Predicted C_{trough} at C6 was used as a measure of rituximab exposure and considered a continuous or categorical covariate.

RESULTS

Analysis population

The dataset comprised 4739 quantifiable serum samples (1777 R-s.c. and 2,962 R-i.v.) from 255 rituximab-treated patients in SAWYER and REACH (Table 1).

Of 255 patients (172 men), 45.1% received R-i.v. only; 54.9% received both R-i.v. and R-s.c. (Table 2). ADA after treatment initiation were detected in 13 (5.1%) patients in SAWYER (not measured in REACH), three in part 1, and six and four, respectively, in the R-i.v. and R-s.c. arms of part 2. BSIZ was log-normally distributed.

PopPK analyses

Base PK model development

Rituximab serum concentrations following i.v. and s.c. dosing were accurately described by a linear two-compartment PopPK model with CL_T (decreased exponentially with time), CL_{inf} , and first-order s.c. absorption, as previously demonstrated. Correlations were added between CL_{inf} and central volume (V_C), and between absorption rate constant (k_a) and

TABLE 2 Summary of covariates

Covariate	Description/level	Study			Missing values ^a
		REACH (BO17072)	SAWYER (BO25341)	Total	
Categorical					
Sex	0: men	14 (66.7%)	158 (67.5%)	172 (67.5%)	NA
	1: women	7 (33.3%)	76 (32.5%)	83 (32.5%)	NA
Race	1: Caucasian, White, Mediterranean	21 (100%)	220 (94.0%)	241 (94.5%)	NA
	3: American Indian or Alaska native	0	3 (1.3%)	3 (1.2%)	NA
	4: other, East Indian, Maori	0	6 (2.6%)	6 (2.4%)	NA
	–99: missing	0	5 (2.1%)	5 (2.0%)	NA
Presence of ADA (HAHA)	0: not detected	0	221 (94.4%)	221 (86.7%)	NA
	1: detected in ≥1 sample	0	13 (5.6%)	13 (5.1%)	NA
	–99: missing	21 (100%)	0	21 (8.2%)	NA
Route	i.v. only	21 (100%)	94 (40.2%)	115 (45.1%)	NA
	s.c. for ≥1 dose	0	140 (59.8%)	140 (54.9%)	NA
Continuous ^b					
N	No. (%)	21 (8.2%)	234 (91.8%)	255 (100%)	NA
BSA	m ²	1.89 ± 0.227 (1.43–2.35)	1.91 ± 0.192 (1.41–2.42)	1.91 ± 0.195 (1.41–2.42)	1 (<1%)
WT	kg	80.4 ± 16.6 (49.9–115)	79.2 ± 13.7 (47.0–124)	79.3 ± 13.9 (47.0–124)	1 (<1%)
BMI	kg/m ²	28.4 ± 5.14 (19–38.8)	27.2 ± 4.18 (16.7–41.1)	27.3 ± 4.27 (16.7–41.1)	1 (<1%)
AGE	years	55.1 ± 9.18 (38–74)	58.7 ± 8.78 (25–78)	58.4 ± 8.85 (25–78)	0
BSIZ	mm ²	5490 ± 3210 (680–16,100)	6960 ± 7880 (100–55,500)	6810 ± 7540 (100–55,500)	51 (20%)
WBC	×10 ⁹ /L	112 ± 110 (11.0–436)	93.4 ± 71.4 (4.03–344)	95.2 ± 75.8 (4.03–436)	39 (15%)
CRCL	ml/min	101 ± 34.7 (46.6–189)	93.7 ± 24.3 (47.6–195)	94.3 ± 25.4 (46.6–195)	37 (15%)
CRCLN ^c	ml/min/1.73 m ²	91.1 ± 25.0 (43.5–149)	84.8 ± 18.2 (45.2–147)	85.4 ± 19.0 (43.5–149)	37 (15%)
BALB	g/L	47.0 ± 5.06 (38.5–55.4)	44.2 ± 4.68 (30.0–67.5)	44.5 ± 4.78 (30.0–67.5)	44 (17%)
BBCE	×10 ⁶ /L	89,300 ± 108,000 (3,500–429,000)	79,000 ± 71,300 (0–453,000)	79,900 ± 74,600 (0–453,000)	84 (33%)
AST	U/L	22.0 ± 9.99 (13.0–59.7)	25.1 ± 11.6 (10.0–100)	24.8 ± 11.5 (10.0–100)	43 (17%)
ALT	U/L	22.1 ± 10.2 (8.0–47.7)	22.6 ± 12.4 (8.0–79.0)	22.5 ± 12.2 (8.0–79.0)	41 (16%)
ALP	U/L	190 ± 78.4 (70.5–415)	92.7 ± 42.6 (33.9–268)	102 ± 55.3 (33.9–415)	43 (17%)
BILI	μmol/L	12.4 ± 5.66 (6.84–29.7)	11.3 ± 5.81 (2.50–41.9)	11.4 ± 5.79 (2.50–41.9)	38 (15%)
HAHAV	Maximum ADA titer	NA	0.178 ± 0.805 (0–6.12)	0.178 ± 0.805 (0–6.12)	21 (8%)

ADA, anti-drug antibodies; ALP, alkaline phosphatase; ALT, alanine aminotransferase; AST, aspartate aminotransferase; BALB, baseline serum albumin; BBCE, B-cell count; BILI, bilirubin; BMI, body mass index; BSA, body surface area; BSIZ, tumor load; CRCL, creatinine clearance; HAHA, human anti-human antibodies; N, number of patients; NA, not applicable or available; NCRCL, normalized creatinine clearance; WBC, white blood cell count; WT, weight.

^aMissing values were imputed as mean values except for BSIZ, where missing values were imputed as –99 or 0.

^bFor continuous covariates, values are those at baseline and are mean ± SD (range) unless stated otherwise.

^cCalculated using Cockcroft–Gault formula; CRCLN = CRCL/BSA.

s.c. bioavailability (F_{SC}). An effect of BSA on clearance and volumes was added.

All model parameters were estimated with good precision (RSE <12%), except for correlation between k_a and F_{SC} (RSE 30.3%). Shrinkage of random effects was low (≤13.4%).²¹ The NONMEM code for the base model is shown in Table S4.

Final PK model

Covariates retained in the final PK model were BSA on clearance and volume parameters (CL_{inf} , CL_T , intercompartmental clearance [Q], V_C , and peripheral volume [V_P]); WBC and BSIZ on CL_T ; BMI on k_a and F_{SC} ; and sex on V_C . PK parameter

TABLE 3 PK parameter estimates for the final covariate model

Parameter		Estimate	RSE (%)	95% CI
k_{des} (1/day)	Θ_1	0.0399	5.19	0.0359, 0.044
CL_T (ml/day)	Θ_2	1550	8.14	1300, 1800
CL_{inf} (ml/day)	Θ_3	207	2.62	196, 217
V_C (ml)	Θ_4	4990	1.82	4820, 5170
V_P (ml)	Θ_5	3700	1.97	3560, 3840
Q (ml/day)	Θ_6	420	3.23	393, 446
k_a (1/day)	Θ_7	0.372	3.86	0.344, 0.4
F_{SC}	Θ_8	0.633	2.52	0.601, 0.664
$CL_{BSA} = Q_{BSA}$	Θ_{14}	1.37	12.3	1.04, 1.7
$V_{C,BSA} = V_{P,BSA}$	Θ_{15}	0.8	11.4	0.622, 0.978
$CL_{T,WBC}$	Θ_{16}	0.223	34.2	0.0737, 0.373
$V_{C,SEXF}$	Θ_{17}	0.909	2.96	0.856, 0.961
$k_{a,BMI}$	Θ_{18}	-1.01	23.8	-1.48, -0.537
$F_{SC,BMI}$	Θ_{19}	-0.465	35.6	-0.789, -0.141
$CL_{T,BSIZ}$	Θ_{20}	0.261	21.1	0.153, 0.369
σ_L	Θ_9	0.81	8.69	0.672, 0.948
σ_H	Θ_{10}	0.134	4.32	0.123, 0.146
σ_{50}	Θ_{11}	6.35	17.5	4.17, 8.54
σ_{17072}	Θ_{12}	1.42	7.6	1.21, 1.63
σ_{CohA}	Θ_{13}	0.568	5.7	0.505, 0.632

Parameter		Estimate	RSE (%)	95% CI	Variability	Shrinkage
ω^2_{Kdes}	$\Omega(1,1)$	0.357	10.3	0.285, 0.428	CV = 59.7%	13.2%
ω^2_{CLT}	$\Omega(2,2)$	0.691	9.4	0.563, 0.818	CV = 83.1%	10.5%
ω^2_{CLinf}	$\Omega(3,3)$	0.106	10.5	0.0839, 0.127	CV = 32.5%	7.6%
$R\omega_{CLinf}\omega_{Vc}$	$\Omega(3,4)$	0.0277	15.7	0.0191, 0.0362	R = 0.47	–
ω^2_{Vc}	$\Omega(4,4)$	0.0323	11.3	0.0251, 0.0394	CV = 18.0%	9.9%
ω^2_{ka}	$\Omega(5,5)$	0.115	17.7	0.0753, 0.156	CV = 34.0%	9.1%
$R\omega_{ka}\omega_{Fsc}$	$\Omega(5,6)$	0.0265	36.4	0.00759, 0.0454	R = 0.37	–
ω^2_{Fsc}	$\Omega(6,6)$	0.0453	19.0	0.0285, 0.0622	CV = 21.3%	7.9%
ω^2_{σ}	$\Omega(7,7)$	0.0929	10.2	0.0743, 0.111	CV = 30.5%	0%
σ^2	$\Sigma(1,1)$	1	Fixed	–	–	2.8%

BMI, body mass index; BSA, body surface area; BSIZ, tumor size at baseline; CI, confidence interval; CL_{BSA} , effect of BSA on clearance; CL_{inf} , non-specific time-independent clearance; CL_T , specific time-dependent clearance; $CL_{T,BSIZ}$, effect of BSIZ on CL_T ; $CL_{T,WBC}$, effect of WBC on CL_T ; CV, coefficient of variation ($100 \times SD$); F_{SC} , absolute subcutaneous bioavailability; $F_{SC,BMI}$, effect of BMI on F_{SC} ; k_a , subcutaneous absorption rate constant; $k_{a,BMI}$, effect of BMI on k_a ; k_{des} , decay coefficient of time-dependent clearance; PK, pharmacokinetic; Q , intercompartmental clearance; Q_{BSA} , effect of BSA on Q ; $R\omega$, correlation of variances; RSE, relative standard error ($100 \times$ standard error/parameter estimate); V_C , central volume; $V_{C,BSA}$, effect of BSA on V_C ; $V_{C,SEXF}$, effect of female sex on V_C ; V_P , peripheral volume; $V_{P,BSA}$, effect of BSA on V_P ; WBC, white blood cell count. ω^2 , interindividual variance (subscripts show the covariates of interest); Σ , residual covariance matrix, Ω , interindividual covariance matrix; σ_L , standard deviations of the exponential residual error at low concentrations; σ_H , SDs of the exponential residual error at high concentrations; σ_{50} , concentrations when the SD of the exponential residual error is equal to $(\sigma_L + \sigma_H)/2$; σ_{17072} , effect of REACH study on residual error (compared with SAWYER Part 2); σ_{CohA} , effect of SAWYER Part 1 on residual error (compared with SAWYER Part 2); σ^2 , residual variance; Θ , NONMEM fixed effect parameter.

estimates of the final model are summarized in Table 3; influence of covariates is illustrated in Table 4. The NONMEM code for the final model is shown in Table S5. The residual variability

was ~ 13% for concentrations above 60 $\mu\text{g/ml}$ ($9 \times \sigma_{50}$), ~ 50% for a concentration of 6.35 $\mu\text{g/ml}$ (σ_{50}), and increased to a maximum of 80% for concentrations near the LLOQ.

TABLE 4 Covariate effects in the final PK model, and parameters of the CPH models

Parameter	Covariate	Reference value	Covariate value	Covariate effect value, % (95% CI)
CL _T , CL _{inf} , Q	BSA, m ²	1.9	1.53	-25.6 (-30.7, -20.1)
			2.23	24.5 (18.1, 31.2)
V _C , V _P	BSA, m ²	1.9	1.53	-15.9 (-19.1, -12.6)
			2.23	13.7 (10.5, 17.0)
V _C	SEX	Male	Female	-9.1 (-14.4, -3.9)
CL _T	WBC, ×10 ⁹ /L	100	11.6	-38.2 (-55.2, -14.7)
			281	26 (7.9, 47)
			400	-52.7 (-65.2, -35.5)
k _a	BMI, kg/m ²	27	27,000	42.3 (23.0, 64.6)
			20.7	30.7 (15.3, 48.1)
F _{SC}	BMI, kg/m ²	27	36.5	-26.2 (-36.0, -14.9)
			20.7	13.1 (3.8, 23.3)
			36.5	-13.1 (-21.2, -4.1)

Covariate	PFS models			
	β	SE	RSE	HR (95% CI)
Log(C _{trough}) model				
Log(C _{trough}), μg/ml	-1.273	0.2596	20.39	0.280 (0.17, 0.47)
Log(BSIZ), mm ²	0.4706	0.2021	42.94	1.601 (1.08, 2.38)
Two-level model				
C _{trough} <32 μg/ml, (yes/no)	2.588	0.427	16.48	13.3 (5.77, 30.7)
Log(BSIZ), mm ²	0.517	0.206	39.87	1.68 (1.12, 2.51)
Three-level model				
C _{trough} <32 μg/ml vs 32–113 μg/ml	2.243	0.4412	19.67	9.42 (3.97, 22.4)
C _{trough} >113 μg/ml vs 32–113 μg/ml	-1.004	0.4694	46.75	0.37 (0.15, 0.92)
Log(BSIZ), mm ²	0.5476	0.216	39.45	1.73 (1.13, 2.64)

β, beta; BMI, body mass index; BSA, body surface area; BSIZ, tumor size at baseline; CI, confidence interval; CL_T, specific time-dependent clearance; CL_{inf}, non-specific time-independent clearance; CPH, Cox proportional hazards; C_{trough}, trough (minimum) serum rituximab concentration; F_{SC}, absolute subcutaneous bioavailability; HR, hazard ratio; k_a, subcutaneous absorption rate constant; PFS, progression-free survival; PK, pharmacokinetic; Q, intercompartmental clearance; RSE, residual standard error; SE, standard error; V_C, central volume; V_P, peripheral volume; WBC, white blood cell count.
Log is a natural log function.

CL_{inf}, Q, V_C, V_P, terminal half-life, k_a, and F_{SC} were in ranges typical for mAbs. High initial CL_T (1550 ml/day), possibly attributable to TMDD, was 7.5 times higher than CL_{inf} and decreased over time (half-life 17.4 days).

Dependence of CL_{inf}, CL_T, and Q on BSA was consistent with allometric scaling, with ~ 25% differences for subjects with low and high BSA versus reference (1.9 m²). Dependence of V_C and V_P on BSA was lower (differences 14–16%). CL_T values influencing initial clearance (c.f. steady-state) were 42% and 26% higher, respectively, in subjects with high BSIZ and WBC, and 53% and 38% lower, respectively, in subjects with low BSIZ and WBC compared with reference values (7000 mm² and 100 × 10⁹ cells/L, respectively). BMI influenced k_a (26% lower in patients with high BMI, and 31% higher for low BMI versus reference [27 kg/m²]). The influence of sex on V_C and

BMI on F_{SC} was minor. All structural parameters and parameters of the interindividual random effects and residual error were estimated with good precision (RSE ≤ 8.1% and < 19.0%, respectively), although correlation between k_a and F_{SC} was estimated with lower precision (RSE 36.4%). Covariate effects were estimated precisely for clearance and volumes (RSE ≤ 12.3%), but with lower precision for CL_T, k_a, and F_{SC}. Shrinkage of the random effects was low (≤ 13.2%).

Covariate model diagnostic plots did not indicate model deficiencies (Figures S2 and S3). Dependencies of random effects on covariates did not show any notable trends unaccounted for by the model. The prediction-corrected VPC simulations indicated good agreement between simulated and observed data, barring slight underestimation of concentrations in the R-s.c. arm of SAWYER part 2

(Figure S4). NPDE plots (Figure S5) confirmed good agreement between the simulated and observed data, with no covariate trends. Potential bias was observed at late time points for NPDE versus time, but no relationship among CL_{inf} , BALB, or albumin time course and response was seen (Figures S6 and S7).

Conditional simulations

Model-based simulations of concentration–time courses of R-i.v. and R-s.c. showed that steady-state was reached by C6 (Figure 1).

Rituximab PKs depended on body size measures (Figure 1, Table 4, Figure S8). CL_{inf} , CL_T , V_C , V_P , and Q increased with BSA. V_C was slightly (9%) lower in women than men. The k_a and F_{SC} decreased with increasing BMI. Conditional simulations summarizing body size dependencies on rituximab exposure (Figure 1) demonstrated that, whereas flat s.c. dosing led to increased differences in exposure (C_{trough} and AUC_τ) between persons with low and high body sizes compared with bodyweight-adjusted i.v. dosing, it maintained C_{trough} and AUC_τ values for all body size groups at levels not lower than those attained with i.v. dosing. C_{trough} and AUC_τ values were 12% higher for i.v. versus s.c. dosing in patients weighing greater than 90 kg; smaller patients had average C_{trough} and AUC_τ values following i.v. dosing ~ 16% and ~ 10% lower, respectively, than with s.c. dosing for patients weighing 60–90 kg. Similar patterns were observed according to BSA tertiles (Figure 1).

CL_T was higher in subjects with higher WBC and BSIZ (Table 3). Presence of ADA in 13 patients in SAWYER had no influence on concentration–time courses.

Exposure–safety and exposure–response analyses

Exposure–safety

There was no apparent link between serum rituximab concentration and SAE frequency (Figure S9). Serum rituximab concentrations for subjects with/without SAEs were similar, and there were no apparent relationships between exposure and SAEs, grade 3 or higher AEs, or neutropenia (Figure S10).

Exposure–Response

There were no differences in exposure between patients with complete response (CR), CR with incomplete blood count

recovery (CRi), or partial response (PR) (Figure 2). Two R-i.v.-treated patients had stable disease. Exposure of R-s.c.-treated patients with PR appeared lower than for those with CR/CRi. Nevertheless, compared with R-i.v., exposure was the same when all patients were analyzed, or slightly higher when only patients who received five or six doses were included. Weight, BSA, WBC, and BSIZ showed no strong correlations with response.

There was a minor trend toward stronger B-cell response with higher exposure for both R-i.v. and R-s.c. (Figure S11). B-cell count declined from baseline to very low levels ($\sim 10 \times 10^6/L$) immediately after starting treatment in the high-exposure group, decreasing further to $2 \times 10^6/L$, with slow increases after treatment end. In the mid-exposure group, B-cell count decreased to very low levels, and more patients had increasing B-cell counts during follow-up. Low-exposure patients had higher B-cell nadirs ($\sim 100 \times 10^6/L$), which took longer to reach than in the other exposure groups. This group had the most patients with values increasing during follow-up.

Analysis of exposure–PFS relationships included 145 patients from SAWYER part 2. Exploratory KM PFS analysis, with patients grouped by exposure category, indicated that the R-i.v. and R-s.c. curves nearly coincide, but PFS of eight (5.5%) patients with C_{trough} less than $32 \mu g/ml$ was shorter than PFS of patients with higher exposure (Figure 3). Individual PK and B-cell profiles for these eight patients are shown in Table S6. When these patients were excluded, there were no pronounced differences in PFS between or within the R-s.c. and R-i.v. arms. Patients with more severe disease (i.e., larger BSIZ) exhibited lower PFS versus patients with milder disease.

PK time course and parameter estimates (CL , CL_{inf} , and k_{des}) were compared graphically among those eight patients and the rest of the population ($n = 137$; Figure S12). In those eight patients, rituximab C_{trough} concentrations were systematically lower than the PopPK model predictions; BSIZ tended to be higher and consequently, CL_T and k_{des} were higher and lower, respectively, compared with the rest of the population (Figure S13; i.e., time needed to saturate this CL_T elimination pathway was longer). In contrast, C_{max} was similar among all patients; C_{max} depends on volumes, which do not depend on patient factors, unlike C_{trough} . The time course of serum albumin over C1–6 did not differ among those eight patients and the rest of the population, nor between responders and nonresponders.

Despite inherent data limitations (single-dose, time-dependent PK, and TMDD), classical ER methodology (multivariate CPH modeling) was used to explore the potential relationship between exposure and PFS. The model with the lowest BIC included $\log(C_{trough})$ as a continuous covariate of PFS (Figure 3, Table 4). This model provided a good description of PFS in all exposure groups,

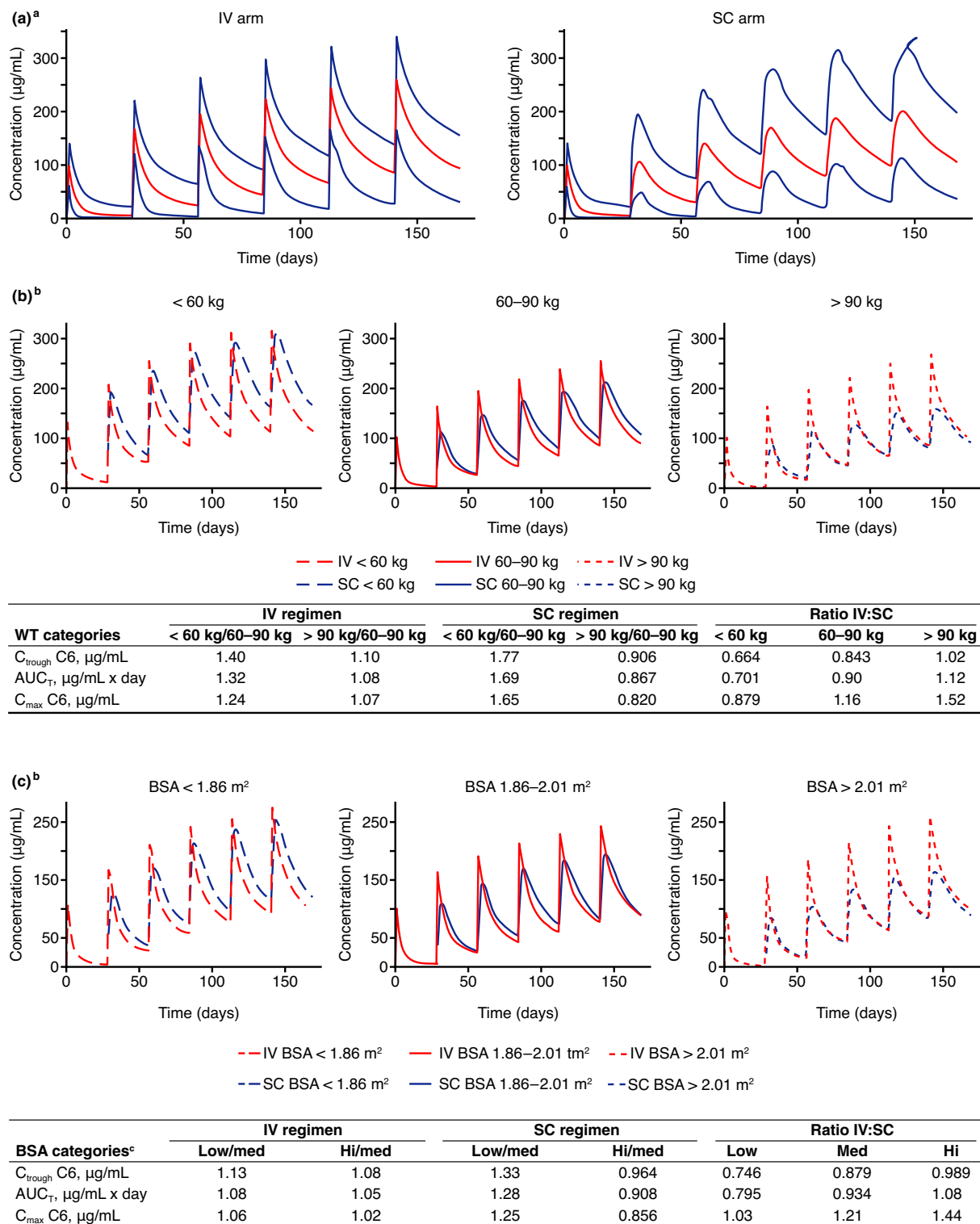


FIGURE 1 Model-based conditional simulations following i.v. and s.c. dosing: (a) overall; (b) by bodyweight categories; (c) by BSA tertile. Concentration–time courses were simulated following i.v. (375 mg/m^2 in C1, followed by 500 mg/m^2 in C2–6) or s.c. dosing (375 mg/m^2 i.v. in C1, followed by 1600 mg s.c. in C2–6). The individual covariates and parameters of 140 subjects from part 2 of SAWYER with available s.c. data were used for simulations. Summary data for ratios of conditional predictions of exposure by bodyweight categories (b) and tertiles of BSA (c) are also shown. AUC_T , area under the curve of serum rituximab concentration versus time for one cycle; BSA, body surface area; C, cycle; C_{max} , maximum serum rituximab concentration; C_{trough} , minimum serum rituximab concentration; WT, weight. ^aMedians are shown in red and 5th and 95th percentiles are shown in blue. ^bMedians of simulated concentrations for each bodyweight category (b) or BSA tertile (c). ^cLow: BSA less than 1.86 m^2 , med (medium): BSA $1.86\text{--}2.01 \text{ m}^2$, hi (high): BSA greater than 2.01 m^2

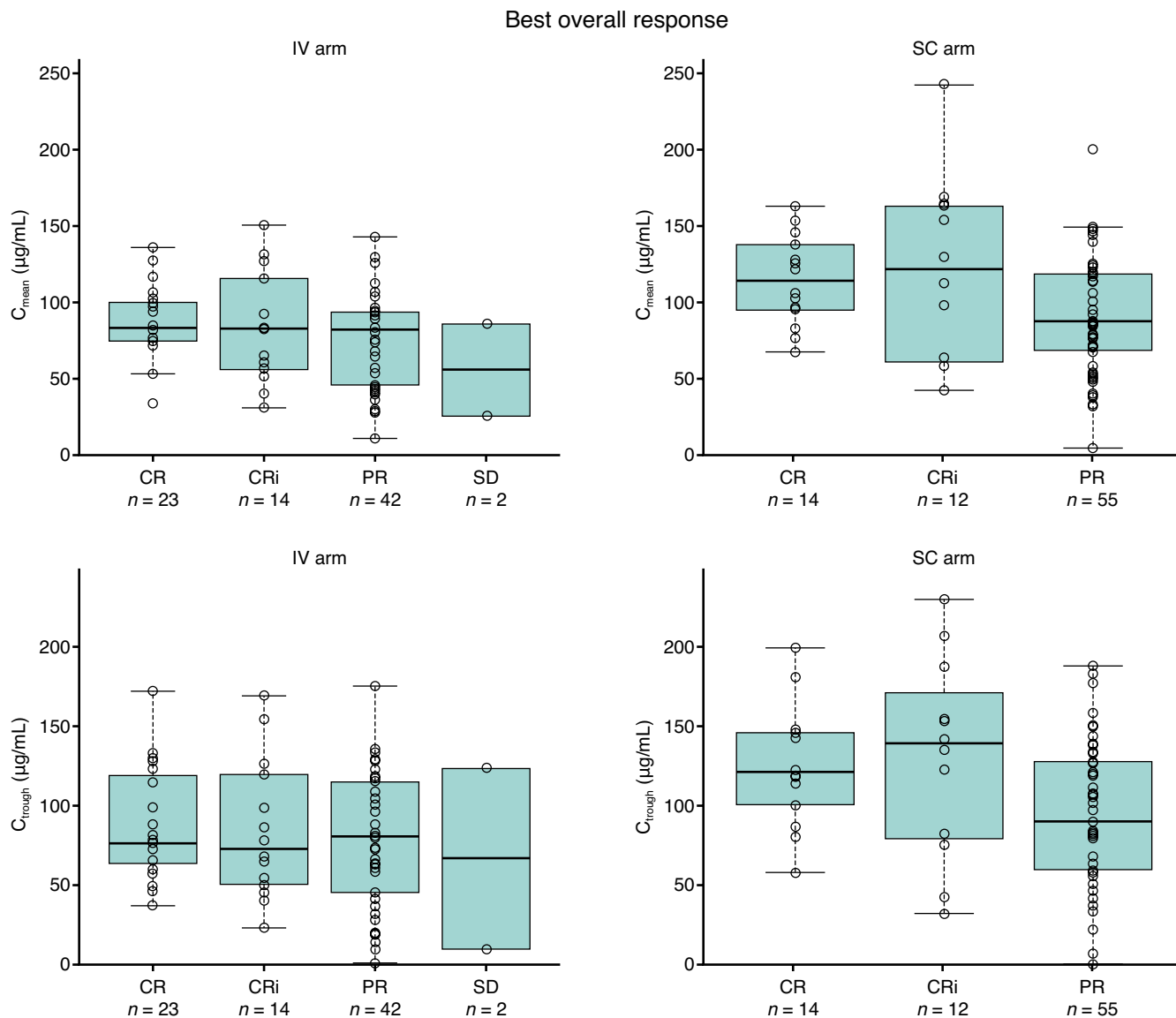


FIGURE 2 Relationship between best overall response and mean and trough serum concentrations for all patients by treatment arm. Black lines in centers of boxes = median values. Boxes indicate IQRs; whiskers indicate $1.5 \times$ IQR; circles show individual values. C_{mean} , mean serum rituximab value; C_{trough} , minimum serum rituximab value; CR, complete response; CRi, complete response with incomplete blood count recovery; IQR, interquartile range; PR, partial response; SD, stable disease. Includes $n = 145$ patients who received all six cycles of rituximab in SAWYER part 2

barring some overestimation for the eight patients with the lowest exposure (Figure S14a,d). Additional models included C_{trough} as a categorical covariate, the first of which had two categories of exposure (C_{trough} less than 32 $\mu\text{g/mL}$ and 32 $\mu\text{g/mL}$ or greater). This model correctly predicted PFS in patients with C_{trough} less than 32 $\mu\text{g/mL}$, as well as in patients from the first and second exposure tertiles, but slightly underestimated PFS in patients with the highest exposure tertile (Figure S14b). Ultimately, a CPH model with three categories of exposure was tested (C_{trough} less than 32 $\mu\text{g/mL}$; C_{trough} 32–113 $\mu\text{g/mL}$; C_{trough} greater than 113 $\mu\text{g/mL}$), which had a slightly higher BIC than the others.

This model correctly predicted PFS in all exposure groups (Figure S14c).

CPH analyses demonstrated no differences in PFS between the R-i.v. and R-s.c. arms. The eight patients with C_{trough} less than 32 $\mu\text{g/mL}$ (of whom 2 received R-s.c. and 6 R-i.v.) had a 13.3-fold (95% CI = 5.76–30.7) higher risk of progression or death than other patients. Two R-i.v.-treated patients had ADA. Among the 137 patients with higher exposure, there was no statistically significant ER relationship, although a trend toward longer PFS with higher exposure was noted; hazard ratio for progression or death was 2.7 times lower (hazard ratio 0.366; 95% CI = 0.146–0.919) in patients with C_{trough}

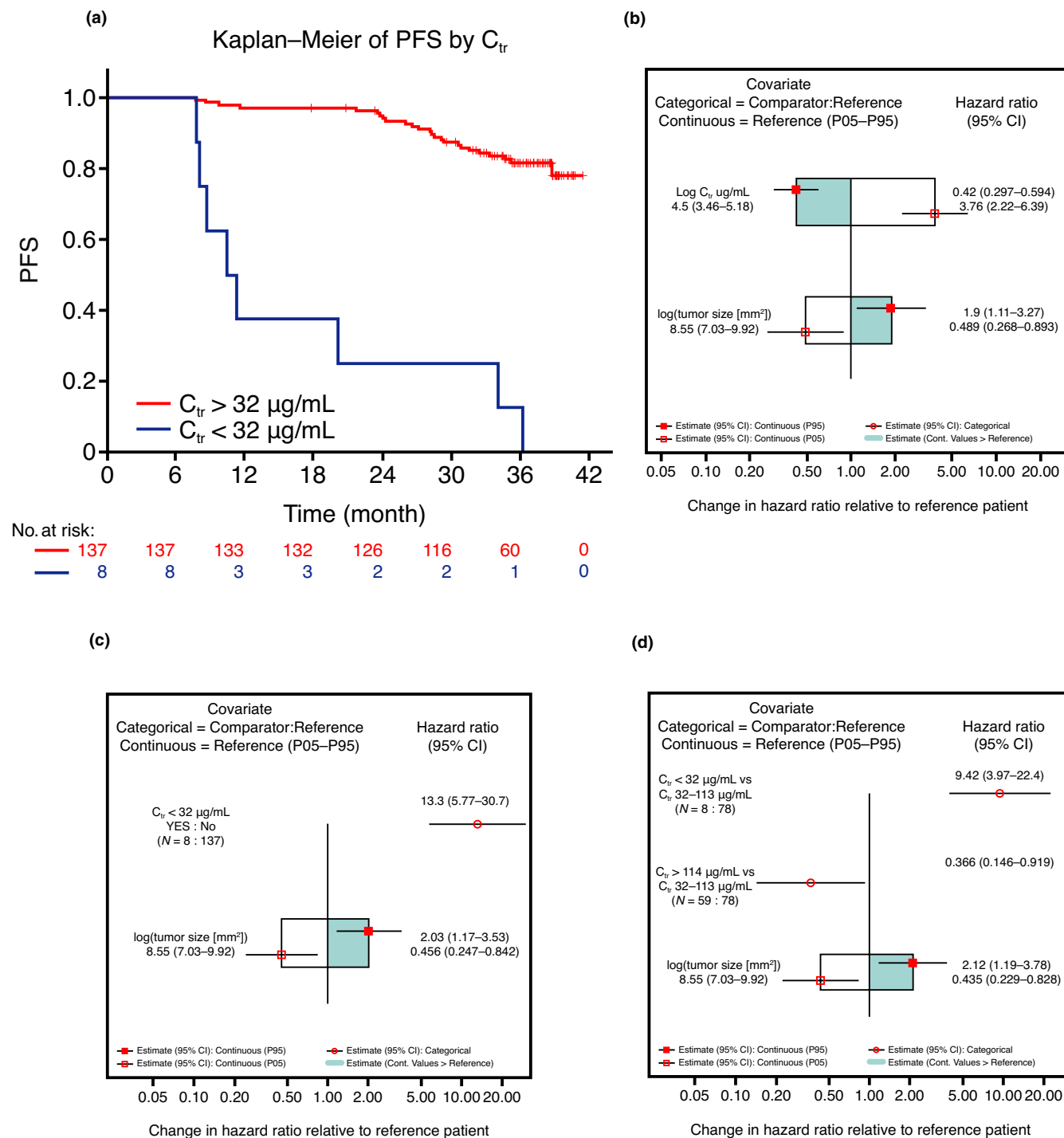


FIGURE 3 Kaplan–Meier plot of PFS for low ($<32 \mu\text{g/mL}$) and high ($\geq 32 \mu\text{g/mL}$) exposure patients in the exposure–PFS analysis (a); multivariate analyses ($\log(C_{trough})$ [b], two- [c] and three-level models [d]^a, respectively) of PFS: covariate effects on the PFS hazard for the CPH models. C, cycle; CI, confidence interval; CPH, Cox proportional hazards; C_{tr} , C_{trough} at the end of C6, patient’s minimum serum rituximab concentration at the end of C6; PFS, progression-free survival. ^aCutoffs of 32 and 113 $\mu\text{g/mL}$ were chosen according to tertile of rituximab exposure

greater than 113 $\mu\text{g/mL}$ versus patients with C_{trough} 32–113 $\mu\text{g/mL}$. BSIZ (independent of C_{trough} ; relationships among BSIZ, WBC, and C_{trough} are shown in Figure S15) had a statistically significant effect on PFS; larger BSIZ increased risk of progression or death (Figure 3, Table 4). Adjusting for BSIZ did not change the association between exposure and PFS.

DISCUSSION

The concentration–time courses of rituximab following i.v. and s.c. administration were accurately described by a two-compartment PK model with time-dependent and time-independent clearances, and first-order s.c. absorption. The

model was consistent with previous PopPK analyses of rituximab,^{14,22} and with the PKs of other B-cell-targeting antibodies (often in a time-dependent manner²³), such as obinutuzumab.²⁴ The time dependency may be related to target depletion and/or changes in target expression levels with time.

Consistent with TMDD, CL_T was influenced by B-cell count and BSIZ at baseline. As target cells are killed, less CD20 target is available for rituximab and CL_T declines (i.e., CL_T initially represents most of total clearance, then CL_{inf} becomes predominant). CL_T was initially 7.5 times higher than CL_{inf} and decreased with time. This decline lagged behind the decrease in peripheral B-cells, which began immediately after administration for the high-exposure tertile, suggesting more time is required to deplete B-cells in tissue.

Clearance and volume parameters of rituximab increased with body size, as expected for an mAb.²⁵ A power function (value of 1.37) was estimated to characterize the effect of BSA on clearance. The higher power value compared with allometric scaling may be due to the narrower BSA range in the current population (1.41–2.42 m²). R-s.c. absorption also depended on body composition, with k_a and F_{sc} decreasing with increasing BMI. These effects may be related to greater thickness and different structure of hypodermis in patients with higher BMI, although this is poorly understood.²⁶ Despite this, flat-dose s.c. administration maintained C_{trough} and AUC_T values for all body size groups at levels not lower than those attained with R-i.v., thereby also achieving full saturation.

The exposure–safety analysis showed no correlation between rituximab exposure and neutrophil counts, occurrence/frequency of SAEs or grade 3 or higher AEs, or occurrence or grade of neutropenia following either administration route.

Patients with PR to R-s.c. had the same rituximab exposure as patients receiving R-i.v., whereas exposure in patients with CR/CRi in the R-s.c. arm appeared to be higher than in the R-i.v. arm. No patients had stable disease in the R-s.c. arm.

Similarly, a minor trend toward stronger B-cell response in higher exposure groups was noted for both R-i.v. and R-s.c., consistent with rituximab's mode of action.

Analysis of the exposure–PFS relationship in patients who received six cycles of rituximab in SAWYER part 2 indicated that: (i) PFS was comparable between treatment routes; (ii) in patients with C_{trough} of at least 32 µg/ml (94.5%; $n = 137$), no statistically significant exposure–PFS relationship was identified, whereas a trend toward longer PFS with higher exposure was observed; (iii) patients with C_{trough} less than 32 µg/ml ($n = 8$) had a higher risk of progression or death than other patients, irrespective of rituximab formulation; and (iv) BSIZ had a statistically significant effect on PFS. Thus, patients with higher baseline tumor burden had increased risk of progression or death.

In the case of TMDD and time-dependent PKs, the application of classical ER methodology may lead to misinterpretation and artificial ER relationships, particularly if only one dose level is considered.^{27–29} In the current analysis, systemic exposure to rituximab (steady-state C_{trough}) is not an independent predictor of response, but rather a function of it. Analysis of the relationship between clinical outcome and exposure is often complicated by the underlying relationship between exposure and treatment response, but also tumor burden, target expression (CD20 for rituximab), disease biology, and treatment resistance. In this case, an apparent ER analysis could be more of a “response”-driven ER, where change in exposure is the consequence of response to treatment rather than the cause of poor clinical outcome. Thus, as previously suggested by Jamois et al.,²⁷ in patients with lower rituximab C_{trough} (less than 32 µg/ml in the current analysis) lower exposure (or higher clearance), could be a consequence of biological factors leading to poorer prognosis (e.g., high rate of mAb internalization or high CD20 expression) rather than the cause of poorer clinical outcome.³⁰ Indeed, previous studies in rituximab and trastuzumab have shown that increasing dose does not necessarily improve outcomes, suggesting the absence of a true ER relationship.^{31–33} Similar findings have been reported for rituximab in other hematological malignancies, such as DLBCL.³⁴

Since the emergence of checkpoint inhibitors (CPIs), cachexia and nutritional status of cancer patients have been extensively discussed as important disease-related factors that could confound ER analyses.^{28,29} With CPI use, clearance and serum albumin evolve with time as the disease progresses. Patients who respond to treatment are less cachexic (higher albumin level) and have lower drug clearance than before treatment. To avoid the confounding effect of change in disease status on PKs, and identify true causal ER relationships, early exposure metrics (e.g., C_{trough} or AUC following first dose) have been utilized, and assessments performed over a wide range of dose levels.^{35–38}

In this analysis, the lower C_{trough} observed in eight patients compared with the overall sample may be related to their tumor burden before treatment initiation, and possibly the presence of ADA. Rituximab's CL_T , which decreased with a half-life of 17.4 days, is associated with TMDD, as reported for other anti-CD20 agents, and is therefore impacted by BSIZ (per the PK model). However, it is not thought to be related to cachexia (no obvious difference in BALB or albumin time course was seen between responders and nonresponders in SAWYER part 2; and no association was observed between BSIZ and BALB). Rituximab's target influenced its PKs as of first dosing (as evidenced by BSIZ and B-cell count effects on CL_T), therefore, consideration of an early metric of exposure in this analysis would not address the uncertainty regarding an ER relationship for rituximab, thus underscoring the limitations of such analyses. The underlying relationship

between exposure and treatment response is complex; emerging methods combining pharmacometrics and artificial intelligence may help support the development of therapeutic mAbs.³⁹

In conclusion, in patients with CLL, rituximab C_{trough} following s.c. administration of 1600 mg during C2–6 is at least equivalent to that achieved with a reference R-i.v. regimen, regardless of body size. There were no differences between R-s.c. and R-i.v. in exposure–safety relationships. The current study highlights the limitations of using classical ER methodology when PKs are time-dependent, exposure is not an independent covariate for predicting response, and when early exposure metrics fail to account for confounding due to the presence of TMDD. Nevertheless, the exposure–efficacy analysis described herein showed that switching from i.v. dosing at 375 mg/m² to a s.c. 1600 mg flat dose does not impair the anti-B-cell activity of rituximab or significantly affect PFS.

ACKNOWLEDGEMENT

Support for third-party writing assistance for this manuscript was provided by Lynda McEvoy, Ashfield MedComms, UK, an Ashfield Health company, funded by F. Hoffmann-La Roche Ltd.

DATA AVAILABILITY STATEMENT

Qualified researchers may request access to individual patient level data through the clinical study data request platform (<https://vivli.org/>). Further details on Roche's criteria for eligible studies are available here (<https://vivli.org/members/ourmembers/>). For further details on Roche's Global Policy on the Sharing of Clinical Information and how to request access to related clinical study documents, see here (https://www.roche.com/research_and_development/who_we_are_how_we_work/clinical_trials/our_commitment_to_data_sharing.htm)

CONFLICT OF INTEREST

E.G. and L.G. were consultants of F. Hoffmann-La Roche Ltd. C.C., N.F., and C.J. are employees of F. Hoffmann-La Roche Ltd. C.J. holds stocks in F. Hoffmann-La Roche Ltd.

AUTHOR CONTRIBUTIONS

E.G., L.G., C.C., N.F., and C.J. wrote the manuscript. E.G., L.G., N.F., and C.J. designed the research. E.G., L.G., C.C., and C.J. performed the research. E.G., L.G., C.J., and N.F. analyzed the data.

REFERENCES

- Salles G, Barrett M, Foà R, et al. Rituximab in B-cell hematologic malignancies: a review of 20 years of clinical experience. *Adv Ther.* 2017;34:2232-2273.
- Hallek M, Fischer K, Fingerle-Rowson G, et al. Addition of rituximab to fludarabine and cyclophosphamide in patients with chronic lymphocytic leukaemia: a randomised, open-label, phase 3 trial. *Lancet.* 2010;376:1164-1174.
- Fischer K, Bahlo J, Fink AM, et al. Long-term remissions after FCR chemoimmunotherapy in previously untreated patients with CLL: updated results of the CLL8 trial. *Blood.* 2016;127:208-215.
- Robak T, Dmoszynska A, Solal-Céligny P, et al. Rituximab plus fludarabine and cyclophosphamide prolongs progression-free survival compared with fludarabine and cyclophosphamide alone in previously treated chronic lymphocytic leukemia. *J Clin Oncol.* 2010;28:1756-1765.
- Davies A, Berge C, Boehnke A, et al. Subcutaneous rituximab for the treatment of B-cell hematologic malignancies: a review of the scientific rationale and clinical development. *Adv Ther.* 2017;34:2210-2231.
- Davies A, Merli F, Mihaljevic B, et al. Pharmacokinetics and safety of subcutaneous rituximab in follicular lymphoma (SABRINA): stage 1 analysis of a randomised phase 3 study. *Lancet Oncol.* 2014;15:343-352.
- Davies A, Merli F, Mihaljević B, et al. Efficacy and safety of subcutaneous rituximab versus intravenous rituximab for first-line treatment of follicular lymphoma (SABRINA): a randomised, open-label, phase 3 trial. *Lancet Haematol.* 2017;4:e272-e282.
- Assouline S, Buccheri V, Delmer A, et al. Pharmacokinetics, safety, and efficacy of subcutaneous versus intravenous rituximab plus chemotherapy as treatment for chronic lymphocytic leukaemia (SAWYER): a phase 1b, open-label, randomised controlled non-inferiority trial. *Lancet Haematol.* 2016;3:e128-e138.
- Assouline S, Buccheri V, Delmer A, et al. Pharmacokinetics and safety of subcutaneous rituximab plus fludarabine and cyclophosphamide for patients with chronic lymphocytic leukaemia. *Br J Clin Pharmacol.* 2015;80:1001-1009.
- FDA. *Highlights of prescribing information: Rituxan Hycela™ (rituximab and hyaluronidase human) injection, for subcutaneous use*; 2021. https://www.genecom/download/pdf/rituxan_hycela_prescribingpdf. Accessed March 24, 2021.
- Rummel M, Kim TM, Aversa F, et al. Preference for subcutaneous or intravenous administration of rituximab among patients with untreated CD20+ diffuse large B-cell lymphoma or follicular lymphoma: results from a prospective, randomized, open-label, cross-over study (PrefMab). *Annals Oncol.* 2017;28:836-842.
- De Cock E, Kritikou P, Sandoval M, et al. Time savings with rituximab subcutaneous injection versus rituximab intravenous infusion: A time and motion study in eight countries. *PLoS One.* 2016;11:e0157957.
- EMA. *MabThera Summary of Product Characteristics*; 2020. https://www.ema.europa.eu/en/documents/product-information/mabthera-epar-product-information_en.pdf.
- Li J, Zhi J, Wenger M, et al. Population pharmacokinetics of rituximab in patients with chronic lymphocytic leukemia. *J Clin Pharmacol.* 2012;52:1918-1926.
- Yano Y, Beal SL, Sheiner LB. Evaluating pharmacokinetic/pharmacodynamic models using the posterior predictive check. *J Pharmacokinetic Pharmacodyn.* 2001;28:171-192.
- Bergstrand M, Hooker AC, Wallin JE, Karlsson MO. Prediction-corrected visual predictive checks for diagnosing nonlinear mixed-effects models. *AAPS J.* 2011;13:143-151.
- Wang DD, Zhang S. Standardized visual predictive check versus visual predictive check for model evaluation. *J Clin Pharmacol.* 2012;52:39-54.

18. Mentré F, Escolano S. Prediction discrepancies for the evaluation of nonlinear mixed-effects models. *J Pharmacokinet Pharmacodyn*. 2006;33:345-367.
19. Brendel K, Comets E, Laffont C, Laveille C, Mentré F. Metrics for external model evaluation with an application to the population pharmacokinetics of gliclazide. *Pharm Res*. 2006;23:2036-2049.
20. Efron B. Missing data, imputation, and the bootstrap. *J Am Stat Assoc*. 1994;89:463-475.
21. Savic RM, Karlsson MO. Importance of shrinkage in empirical bayes estimates for diagnostics: problems and solutions. *AAPS J*. 2009;11:558-569.
22. Yin A, Li J, Hurst D, Visich J. Population pharmacokinetics (PK) and association of PK and clinical outcomes of rituximab in patients with non-Hodgkin's lymphoma. *J Clin Oncol*. 2010;28:e13108.
23. Levi M, Li J, Frey N, et al. Characterization of the time-varying clearance of rituximab in non-Hodgkin's lymphoma patients using a population pharmacokinetic analysis. American Conference on Pharmacometrics; 2005.
24. Gibiansky E, Gibiansky L, Carlile DJ, Jamois C, Buchheit V, Frey N. Population pharmacokinetics of obinutuzumab (GA101) in chronic lymphocytic leukemia (CLL) and non-Hodgkin's lymphoma and exposure-response in CLL. *CPT Pharmacometrics Syst Pharmacol*. 2014;3:e144.
25. Ling J, Zhou H, Jiao Q, Davis HM. Interspecies scaling of therapeutic monoclonal antibodies: initial look. *J Clin Pharmacol*. 2009;49:1382-1402.
26. Richter WF, Bhansali SG, Morris ME. Mechanistic determinants of biotherapeutics absorption following SC administration. *AAPS J*. 2012;14:559-570.
27. Jamois C, Gibiansky E, Gibiansky L, et al. Role of obinutuzumab exposure on clinical outcome of follicular lymphoma treated with first-line immunochemotherapy. *Br J Clin Pharmacol*. 2019;85:1495-1506.
28. Dai HI, Vugmeyster Y, Mangal N. Characterizing exposure-response relationship for therapeutic monoclonal antibodies in immuno-oncology and beyond: Challenges, perspectives, and prospects. *Clin Pharmacol Ther*. 2020;108:1156-1170.
29. Turner DC, Kondic AG, Anderson KM, et al. Pembrolizumab exposure-response assessments challenged by association of cancer cachexia and catabolic clearance. *Clin Cancer Res*. 2018;24:5841-5849.
30. Cartron G, Blasco H, Piantaud G, Watier H, Le Guellec C. Pharmacokinetics of rituximab and its clinical use: thought for the best use? *Crit Rev Oncol*. 2007;62:43-52.
31. Lugtenburg PJ, de Nully Brown P, van der Holt B, et al. Randomized phase III study on the effect of early intensification of rituximab in combination with 2-weekly CHOP chemotherapy followed by rituximab or no maintenance in patients with diffuse large B-cell lymphoma: Results from a HOVON-Nordic Lymphoma Group study. *J Clin Oncol*. 2016;34:7504.
32. Murawski N, Pfreundschuh M, Zeynalova S, et al. Optimization of rituximab for the treatment of DLBCL (I): dose-dense rituximab in the DENSE-R-CHOP-14 trial of the DSHNHL. *Annals Oncol*. 2014;25:1800-1806.
33. Kågedal M, Claret L, Marchand M, et al. Herceptin in HER2-positive gastric cancer: Evaluation of exposure-response with two dose levels. Population Approach Group Europe 2017; Abstract 7329; <https://www.page-meeting.org/?abstract=7329>.
34. Chiappella A, Martelli M, Angelucci E, et al. Rituximab-dose-dense chemotherapy with or without high-dose chemotherapy plus autologous stem-cell transplantation in high-risk diffuse large B-cell lymphoma (DLCL04): final results of a multicentre, open-label, randomised, controlled, phase 3 study. *Lancet Oncol*. 2017;18:1076-1088.
35. Wang Y, Booth B, Rahman A, Kim G, Huang SM, Zineh I. Toward greater insights on pharmacokinetics and exposure-response relationships for therapeutic biologics in oncology drug development. *Clin Pharmacol Ther*. 2017;101:582-584.
36. Diao L, Meibohm B. Pharmacometric applications and challenges in the development of therapeutic antibodies in immuno-oncology. *Curr Pharmacol Rep*. 2018;4:285-291.
37. Wang X, Feng Y, Bajaj G, et al. Quantitative characterization of the exposure-response relationship for cancer immunotherapy: a case study of nivolumab in patients with advanced melanoma. *CPT Pharmacometrics Syst Pharmacol*. 2017;6:40-48.
38. Liu C, Yu J, Li H, et al. Association of time-varying clearance of nivolumab with disease dynamics and its implications on exposure response analysis. *Clin Pharmacol Ther*. 2017;101:657-666.
39. Chaturvedula A, Calad-Thomson S, Liu C, Sale M, Gattu N, Goyal N. Artificial intelligence and pharmacometrics: Time to embrace, capitalize, and advance? *CPT Pharmacometrics Syst Pharmacol*. 2019;8:440-443.

SUPPORTING INFORMATION

Additional supporting information may be found online in the Supporting Information section.

How to cite this article: Gibiansky E, Gibiansky L, Chavanne C, Frey N, Jamois C. Population pharmacokinetic and exposure-response analyses of intravenous and subcutaneous rituximab in patients with chronic lymphocytic leukemia. *CPT Pharmacometrics Syst. Pharmacol*. 2021;10:914-927. <https://doi.org/10.1002/psp4.12665>